

APPLICATION OF ETHALINE DEEP EUTECTIC SOLVENT FOR DISSOLUTION OF GOLD IN SULFIDIC REFRACTORY ORE UNDER VARYING pH

¹Jeanette Karen A. FAIGAL, ¹Christopher Welbourne B. FERRER, ¹Lorenzo Jon M. VILLALOBOS, ²Zyrah Gwen I. SUAYBAGUIO, ³May Anne E. MATA, ^{1,2}Gernelyn T. LOGROSA

¹College of Engineering and Architecture, Mapúa Malayan Colleges Mindanao, Davao City, Philippines, cea@mcm.edu.ph

²Office for Research Development and Innovation, Mapúa Malayan Colleges Mindanao, Davao City, Philippines, research@mcm.edu.ph

³University of the Philippines Mindanao, Mintal, Davao City, Philippines, or upmindanao@up.edu.ph

<https://doi.org/10.37904/metal.2024.4911>

Abstract

Conventional extraction methods like cyanidation face significant challenges with refractory ores, prompting the need for more sustainable alternatives to gold extraction and its metal production. This study evaluates the application of Ethaline, a deep eutectic solvent (DES) composed of choline chloride and ethylene glycol, for dissolving gold from sulfidic refractory ores under varying pH conditions. Ethaline DES, characterized by its non-toxic and biodegradable properties, emerges as a promising solution.

Experiments were conducted at three pH levels: 4 (acidic), 7 (neutral), and 10 (basic). Ore samples were treated with Ethaline DES mixed with iodine as an oxidant, and gold dissolution was monitored over a 72-hour period. The results revealed that the neutral pH condition achieved the highest gold dissolution rate, peaking at 56.7% at 48 hours, followed by the basic and acidic conditions. These findings underscore the critical role of pH in optimizing the dissolution process and highlight the potential of Ethaline DES as a green solvent for gold extraction, promoting more sustainable mining practices and reducing environmental impact.

Keywords: Gold leaching, metal extraction, DES, ethaline, green technologies, refractory ore

1. INTRODUCTION

Gold's significance in human culture and technology has grown historically, initially utilized as the first form of currency due to its high value. Gold's unique thermochemistry properties such as being exceedingly malleable, ductile, and resistant to corrosion and oxidation have paved the way for its application in technology and medicine [1-3].

Gold extraction faces significant challenges due to the depletion of easily accessible free-milling gold ores, shifting the focus towards more complex refractory ores. These ores often contain gold locked within sulfide minerals, making extraction difficult and less efficient using conventional methods like cyanidation [4-7]. The environmental impact of gold mining, especially the use of cyanide and mercury in the extraction process, poses severe environmental and health risks, highlighting the need for more sustainable and less harmful extraction methods [8-10]. This has sparked interest in greener solvents like Ionic Liquids (ILs) and Deep Eutectic Solvents (DESs) for alternative leaching applications. ILs, while versatile, can be toxic, expensive, and not suitable for large-scale use, positioning DESs, particularly those based on non-toxic and biodegradable components like choline chloride and ethylene glycol, popularly known as Ethaline as preferable alternatives. [11-13]. It is especially effective in the dissolution of gold from sulfidic refractory ores, a process that is often challenging with traditional methods [14].

Ethaline facilitates the extraction of gold through a mechanism that involves the formation of complexes with gold ions, enhancing the solubility and recovery. This process is not only more environmentally friendly but also reduces reliance on harsh chemicals and high-energy conditions typically associated with gold leaching. Studies have shown that Ethaline, when combined with iodine, can selectively extract gold by breaking down the ore matrix, which traditionally impedes the leaching process [15-17]. Despite the characterization of Ethaline as generally neutral to alkaline within the observed pH range of 7-8, several factors can induce fluctuations in its pH. These influences include impurities in starting materials: the presence of acidic or basic functional groups in either ChCl or EG, used as starting materials, can alter the overall pH of the Ethaline mixture. Meanwhile, temperature is also a variable, while subtle, can have an impact on the ionization of ChCl and EG, potentially leading to slight pH shifts [18].

Designing processes for gold recovery requires careful consideration of the pH dependence of gold dissolution. Maximizing gold dissolving rates, cutting down on reagent usage, and lessening environmental effects are dependent on pH control [19, 20]. On the other hand, the pH of non-aqueous mixtures like Ethaline, are usually uncontrolled due to its negligible acidity or alkalinity. However, on reactions or processes like in this study where Ethaline is utilized as a solvent, the pH of the reaction mixture may be substantial, depending on the specific chemistry employed [21]. Hence, this paper focuses on evaluating the performance of DES, particularly Ethaline, across various pH environments, with a focus on its application in the leaching of refractory gold ore. Recognizing the significant influence of pH on DES behavior and effectiveness, this research aims to systematically assess how pH conditions affect the dissolution kinetics and efficiency of gold extraction using DES.

2. MATERIALS AND METHODS

2.1 Ore composition

The ore concentrate used in this study was obtained from Apex Mining Co., Inc. Gold was analyzed by atomic absorption spectroscopy (AAS) giving a concentration of 9.64 g/t. Mineralogical analysis using XRD and Mineral Liberation Analyzer was used to determine the mineral phases of the two major ore types of the samples. Shown in **Table 1** is different mineral composition of the ore in wt%.

Table 1 Mineralogical composition of mixed gold concentrate (wt%)

Mineral composition	Content
FeS ₂	29.84
SiO ₂	48.03
CuFeS ₂	2.82
ZnFeS ₂	1.12
ClO ₂	0.59
KAl ₂ (AlSi ₃ O ₁₀)(F,OH) ₂	0.77
KAlSi ₃ O ₈	1.91
KAl ₂ (AlSi ₂ O ₁₀)(F,OH) ₂	11.04
Other Minerals	3.87

2.2 Leaching with Ethaline DES

The Ethaline deep eutectic solvent (DES) was synthesized by mixing choline chloride (HBA) and ethylene glycol (HBD) in molar ratios of 1:1. The resultant mixtures underwent heating at 80 °C and stirring speed of 300 revolutions per minute (rpm) for a duration of 2 hours until a homogenous and transparent phase is reached. 5 grams of the ore was added to 75 ml of the prepared Ethaline DES solution mixed with 15 ml of 1M iodine as oxidant (solid to liquid ratio of 1:15).

The pH of the experimental setups varied into different pH level, specifically pH 4, 7, and 10. These experimental setups were set on an elevated temperature of 50 °C using a 500 ml beaker, and continuously stirred at 300 rpm. All the experimental setups were equipped with a pH, ORP meter and a thermometer. Changes in the pH, oxidation-reduction potential (ORP), and temperature of the solution were systematically monitored at hourly intervals for the initial 6-hour period. Subsequently, these parameters were observed at intervals until the 72-hour leaching period. Data collected from the monitoring process were systematically logged and observed for fluctuations or changes in the solution's parameters over time. Aliquots were taken every 6 hours during the first 24 hours of the experimental run, then every 12 hours at the second 24 hours of the run, and lastly, at the 72nd hour of the experimental run.

2.3 Computational thermochemical calculations

The molecular structures of the proposed gold complexes with the ligands of EG were generated using GaussView. The input file of the generated complexes containing its initial parameters is imported to Gaussian 09W. Gaussian 09W processes the input file to generate the output file containing the output molecular structure and the interpolated Gibbs energy, LUMO-HOMO energy gap, and other thermochemical data needed to support theoretical and experimental data.

3. RESULTS AND DISCUSSION

3.1 Gold dissolved

Each experimental run with different controlled pH level was done in triplicates, thus in every data point that is shown at the leaching time is a data set comprised of the minimum, maximum, and mean of the % Au dissolved.

The results showed that the dissolution of gold varied across acidic, basic, and neutral conditions and is presented in interval plots below.

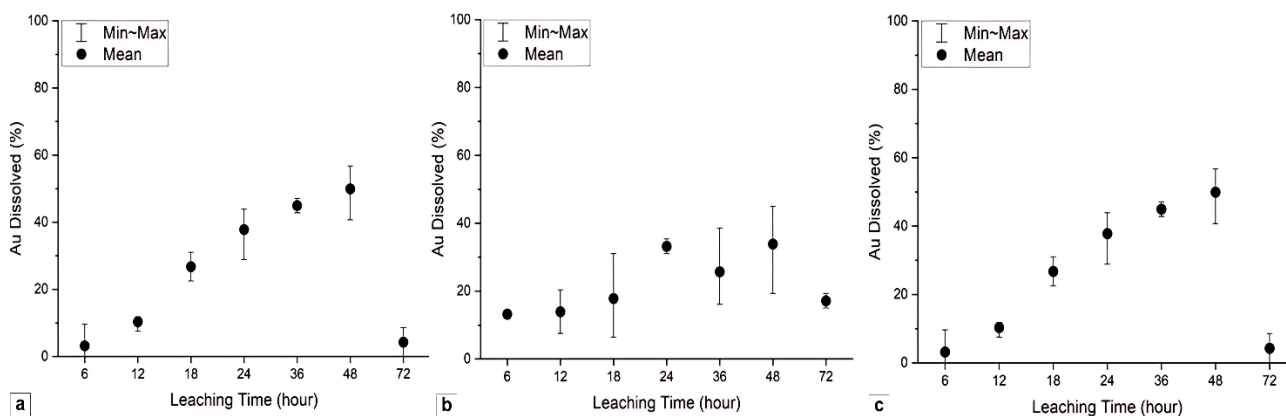


Figure 1 (a) Interval plot for % Au dissolved in an acidic environment; **(b)** Interval plot for % Au dissolved in a basic environment; **(c)** Interval plot for % Au dissolved in a neutral environment

In an acidic environment, the percentage of dissolved gold peaked at the 36th hour with an upper limit value of 42.8% as observed in **Figure 1(a)**. Notably, a fluctuating trend of % Au dissolved in the leaching system subjected to an acidic environment. Meanwhile, in the leaching system adjusted to a basic environment, the percentage of dissolved gold peaked at the 48th hour with an upper limit value of 44.9% and mean value of 33.9%. As can be observed in **Figure 1(b)**, there is an increasing trend of % Au dissolved between the upper limits as the experimental run approaches the 48th hour. Similar to the system adjusted to a basic environment, the percentage of dissolved gold peaked at the 48th hour in a neutral environment and has an upper limit value of 56.7% and mean value of 50.0%, as can be observed in **Figure 1(c)**. There is an increasing trend of % Au dissolved both with the upper limit and means of data points as the experimental run approaches the 48th hour.

Previous studies employing ChCl-based DES has often necessitated extended operating times, exceeding 24 hours [22]. In this study, the peak dissolved gold was found between 24 to 48 hours of all setups and exhibited highest dissolution during the 48th hour of the leaching setup adjusted to a neutral pH. The experimental data still relates with previous sources, such that after the results would peak between the 24th and 48th hour there would be a decline on the dissolution percentage.

3.2 Changes in pH-ORP values

The leaching systems ORP values and pH values prior adjustment to acidic, basic, and neutral environments were logged at specific time intervals; graphical representation of the values is illustrated in **Figure 4, 5 and 6**. The leaching experiments were done in triplicate across various pH environments and each setup was denoted as follows in the graphs: pH 4-A, pH 4-B, pH 4-C, and so forth..

3.2.1. Acidic Ethaline DES leaching system pH and ORP monitoring monitored pH

The monitored pH values of the leaching system adjusted periodically to achieve an acidic environment is shown in **Figure 2(a)**, erratic pH behavior is observed due to the continuous addition of acetic acid to maintain an acidic environment. A notable increase in pH is observed at the 36th hour as it approaches to a near-neutral pH, followed by stabilization to acidic conditions until the end of leaching. Meanwhile the ORP values monitored from the same acidified leaching system in **Figure 2(b)** showed changes in connection with the pH values, with correlation coefficient of 0.7046 as calculated through Pearson correlation analysis. ORP dropped as low as 17 mV in the first two hours as the pH was adjusted to an acidic range. The ORP increased at the 12th hour and peaked with a value of 363 mV by the 64th. pH-ORP trend observed in the monitoring aligns with observed % Au dissolved, where low gold dissolution corresponded with a dip in ORP values for the first 18 hours, while the highest % Au dissolved of 42.8% coincided with the higher ORP values.

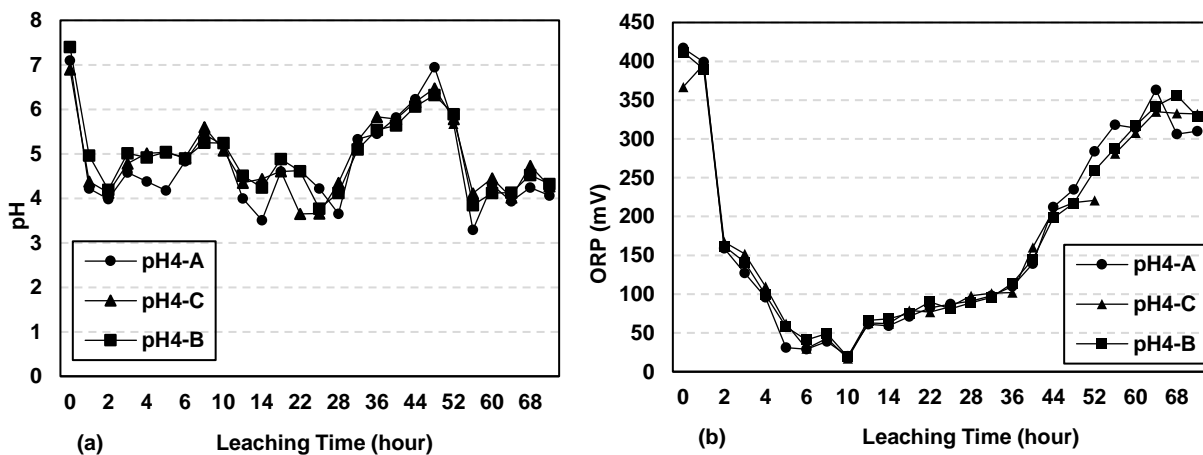


Figure 2 (a) pH values during monitoring of leaching system prior to adjustment to acidic environment; **(b)** ORP values of leaching system in acidic environment

3.2.2. Basic Ethaline DES leaching system pH and ORP monitoring monitored pH

Methylamine was added to leaching setups to observe its behavior in a basic environment. pH reached values between 8.37 to 9.32 as illustrated in **Figure 3(a)** during the first hour and continued to fluctuate peaking between 9.15 and 9.79 by the 5th hour. However, a pronounced decline occurred between the 18th and 22nd hours, where pH dropped to as low as 5.92 (pH 4-B). Despite immediately adjusting the monitored pH to the desired pH of 10 the values generally trended downward, around the range of 5-8. % Au dissolved for the setups set at a basic pH averaged only 22.4%, with a peak value observed during the 48th hour at 37.5%. Complimenting the pH monitoring, the ORP showed significant variations as well. At the 24th hour, high ORP values coincided with peak % Au dissolved across all setups. Conversely, lower ORP values, such as those observed around the 6th and 12th hours, correspond to lower gold dissolution rates.

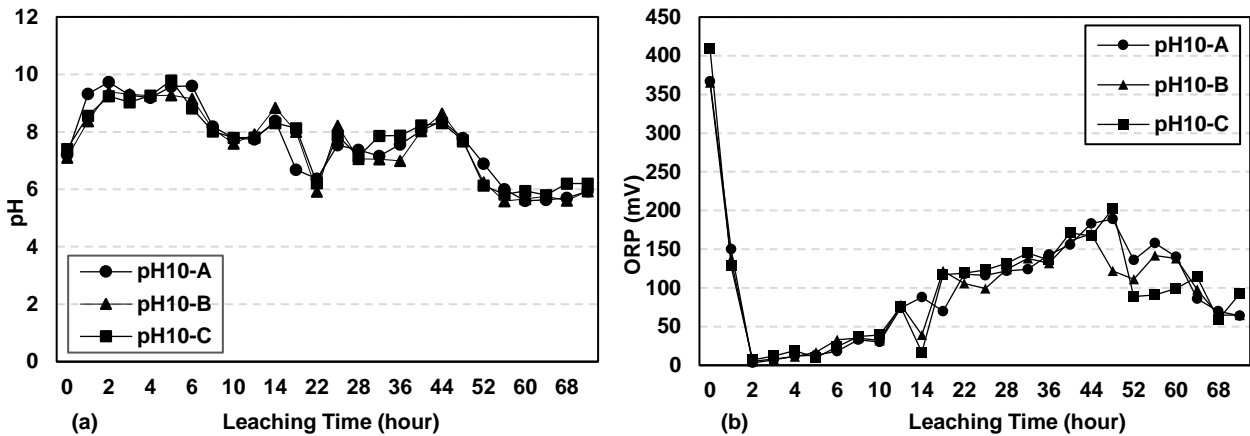


Figure 3 (a) pH values during monitoring prior to adjustment to pH 10; **(b)** ORP values of leaching system in basic environment

In the leaching setup with a neutral pH environment shown in **Figure 4(a)**, pH values fluctuated throughout the 72-hour period. Notably, all setups showed a decline in pH at the 22nd hour, reaching as low as 6.88 and 6.34. Trends indicate periodic rise and dips, without a consistent directional trend. Concurrently, ORP values in **Figure 4(b)** began in the 411-420 range, generally decreased over time but showed occasional peaks, with setups maintained in near-neutral pH achieved the highest overall ORP values compared to other pH environments.

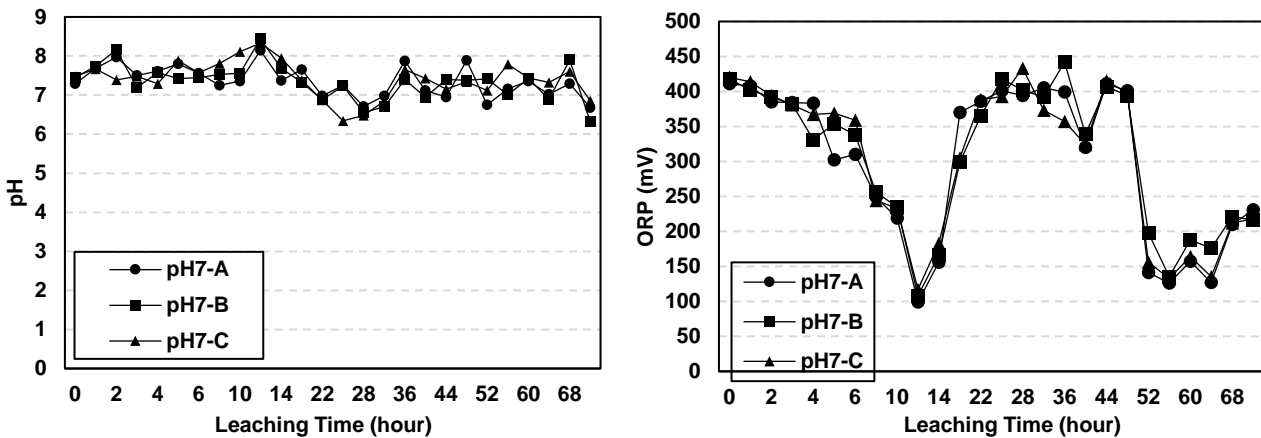


Figure 4 (a) Monitored pH values during monitoring prior to adjustment to pH 7; **(b)** ORP values in neutral environment

3.3 Interpolation and prediction of gold dissolution in various pH environments

The mean values of % Au dissolved at acidic, neutral and basic environments were interpolated using MATLAB's interp1 function, capable of performing one-dimensional interpolation for vector data. This allowed to predict the % Au dissolved at leaching periods not explicitly measured in the experiments. The interpolated data is illustrated in **Figure 5 a)**, **(b)** and **(c)** representing the pH 4, pH 7, and pH 10 environments, respectively.

A 4th-degree polynomial is fitted to the interpolated data to model dissolution behavior over time. The polynomial functions derived for each pH conditions are as follows (**Equations 1-3**):

$$\text{pH 4:} \quad (-1.755 \times 10^{-5})t^4 + (2.598 \times 10^{-3})t^3 - 0.1368t^2 + 3.166t - 5.105 \quad (1)$$

$$\text{pH 7:} \quad (5.226 \times 10^{-7})t^4 - (2.005 \times 10^{-4})t^3 + (2.356 \times 10^{-3})t^2 + 0.820t - 6.742 \quad (2)$$

$$\text{pH 10:} \quad (1.23 \times 10^{-5})t^4 - (2.267 \times 10^{-3})t^3 + 0.1002t^2 - 0.03868t - 4.9298 \quad (3)$$

The fitted polynomial model computed optimal % Au dissolved and corresponding leaching time for each pH environment. The results indicated that in an acidic environment, maximum % Au dissolved of 35.9% is predicted to be obtained at 44.5 hours. For the neutral environment, the highest gold dissolution of 50.5% is projected to be achieved at 42.5 hours, while in a basic environment, the peak gold dissolution of 32.3% is expected to be reached after 45 hours. These results highlight that a near-neutral environment not only yields highest % Au dissolved but also achieves this in the shortest time frame.

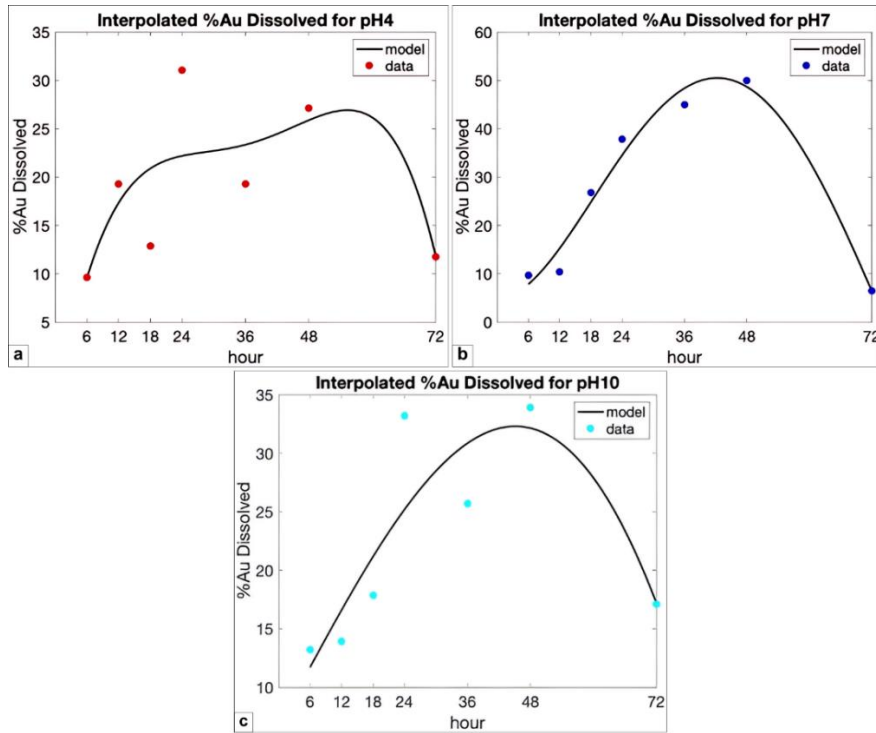


Figure 5 (a) Visualization of interpolated data for DES leaching in acidic environment; **(b)** neutral environment; **(c)** the basic environment

3.4 Stability of Gold Complexes and Thermodynamic Considerations

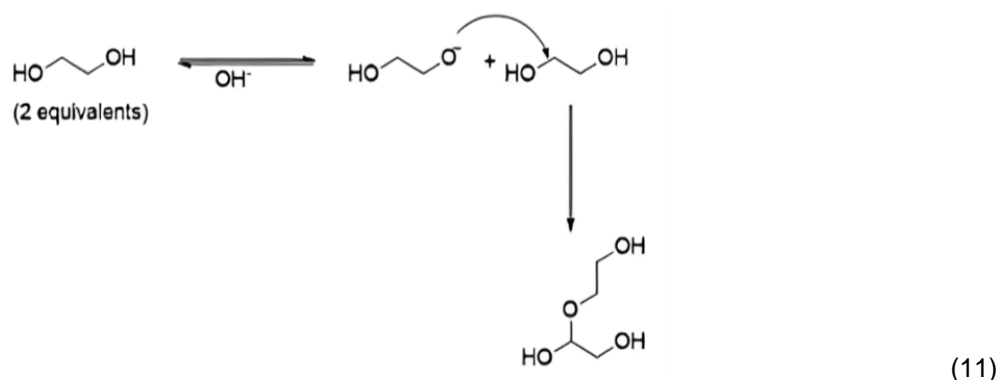
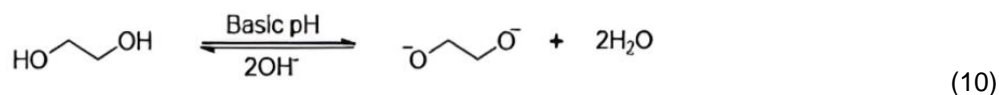
The mean values of % Compared to an aqueous ionic liquid-chlorine electrolyte, Ethaline induces a more vigorous reaction on the anodic dissolution of gold. This disparity is likely attributed to the high concentration of chloride ions in Ethaline. Furthermore, the addition of water enhances the anodic dissolution of gold, corroborating the observed discrepancies in reaction rates. The findings were used to develop a potential chemical equation to describe the electrochemical oxidation mechanism of the gold electrodes in Ethaline (**Equations 4-8**) [24]:



Within an Ethaline solution, the diol component EG ($\text{CH}_2\text{OH}-\text{CH}_2\text{OH}$ or 1,2-ethanediol) can deprotonate at both ends with its two hydroxyl groups relatively, forming either the singly charged anion ($^-\text{OCH}_2-\text{CH}_2\text{O}^-$) or the doubly charged dianion $[\text{C}_2\text{H}_4\text{O}_2]^{2-}$ under basic pH conditions (as depicted in reaction 9) [2].



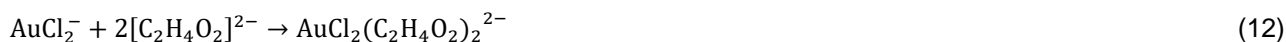
Similar to a pyrite dissolution study by Teimouri [25], the present study found the effect of varying pH levels including 4, 7 and 10, which revealed that a slightly basic pH yielded the maximum Au dissolution efficiency within the Ethaline medium. This observation might be attributed to the likelihood of the EG molecule, containing a carbonyl functional group (which acts as an electrophile), to undergo further transformations beyond values between slightly basic to basic, as represented by reactions (**Equations 10 and 11**), wherein water or a glycerol compound is formed in larger amounts of basicity. This observation is further supported by the study's results where pH level 7 obtained the maximum amount of gold dissolved in average (49.96%), followed by pH 10 (33.87%). This aligns with the previous study [25] which showed that increasing pH above 8 also had a reverse effect on the pyrite extraction, reducing it from 23.6% at pH 8 to only 13.8% at pH 12.



3.4.1 Theoretical Gibbs energy using computational DFT

In this study, density functional theory (DFT) was employed to understand and design ligand-metal complexes. DFT provides insights into the geometry and stability of various complexes, for instance, the Gibbs free energy (ΔG) serves as an indicator for the feasibility of forming the proposed coordination complexes [26]. In the context of the present study investigating gold complexes, the DFT method was employed in conjunction with the Becke, 3-parameter, Lee–Yang–Parr (B3LYP) hybrid functional and the Los Alamos National Laboratory 2-Double Zeta (LANL2DZ) basis set, to execute various thermochemical calculations based on the job type, Frequency. Specifically, B3LYP combines Hartree-Fock exchange with DFT exchange-correlation functionals, while LANL2DZ serves as an effective core potential (ECP), simplifying core electron treatment while accurately representing valence electrons. [27].

Essentially, before initiating the DFT calculations, critical parameters such as molecular geometry, charge, and spin multiplicity are specified. Below are proposed chemical reactions (**Equations 12-15**) between AuCl_2^- and AuCl_4^- ions, along with $\text{C}_2\text{H}_4\text{O}_2^{2-}$ and Cl^- ions, which can lead to the formation of various coordination complexes with different structural arrangements.



The DFT method utilized these reactions to interpolate each of their ΔG values and other thermochemical values. The lowest and the only negative ΔG value is obtained by the complex, $\text{AuCl}_2(\text{C}_2\text{H}_4\text{O}_2)_2$, which is formed from the reactants, AuCl_2^- and $\text{C}_2\text{H}_4\text{O}_2$. The ΔG value of the reactants and products is the sum of their total electronic energy (ε_0) and the thermal correction to Gibbs free energy (G_{corr}) (**Equations 16**).

$$\Delta G = \sum \Delta G(\varepsilon_0 + G_{\text{corr}})_{\text{products}} - \Delta G(\varepsilon_0 + G_{\text{corr}})_{\text{reactants}} \quad (16)$$

The calculation for the reaction of the $\text{AuCl}_2(\text{C}_2\text{H}_4\text{O}_2)_2$ complex is written below (17-18),

$$\Delta G = \sum \Delta G(-618.1113756) - \Delta G(2 * (-226.2262482) + (-165.573846)) \quad (17)$$

$$\Delta G = -0.0850332 \text{ eV} \quad (18)$$

A negative ΔG value signifies an exothermic process, energy being released in this case translates to a higher thermodynamic stability for the formed complexes compared to the initial reactants. The magnitude of the negative ΔG value directly correlates to the strength of the thermodynamic driving force for complex formation. The negative ΔG values quantify the inherent tendency of these complex formation reactions to proceed without the need for external energy input [28]. This stands in contrast to the positive ΔG values observed in **Table 2**, which indicate non-spontaneous reactions under those conditions.

Table 2 Au complexes and their corresponding spin multiplicity, Gibbs energy of formation, and LUMO-HOMO energy gap

Au complex	Spin multiplicity	Gibbs free energy (eV)	LUMO-HOMO gap (eV)
$\text{AuCl}_2(\text{C}_2\text{H}_4\text{O}_2)_2^{2-}$	2	-0.0850332	0.02299
$\text{AuCl}_4(\text{C}_2\text{H}_4\text{O}_2)_2^-$	1	1.1267559	0.02021
$[\text{AuCl}_2(\text{Cl})_4]^{2-}$	2	0.3775122	0.03538
$[\text{AuCl}_4(\text{Cl})_4]^-$	1	0.6525955	0.04537

Generally, the investigated complexes exhibit a very small energy gap between the Lowest Unoccupied Molecular Orbital (LUMO) and Highest Occupied Molecular Orbital (HOMO), except for the $[\text{AuCl}_2(\text{Cl})_4]^{2-}$ complex. LUMO-HOMO gap quantifies the energetic favorability of electron movement within a molecule, directly impacting its electrical transport properties. Molecules with a smaller gap typically demonstrate a greater ease of electron transfer. This characteristic can be linked to enhanced reactivity for specific reaction types in the study, particularly the deprotonation of ethylene glycol or other processes (e.g., oxidation) where electrons are readily removed from the HOMO [29].

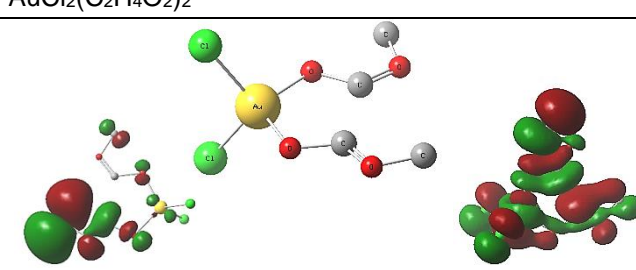
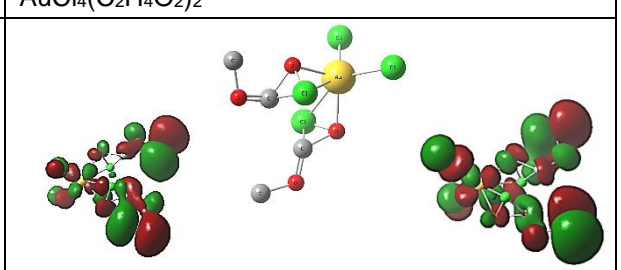
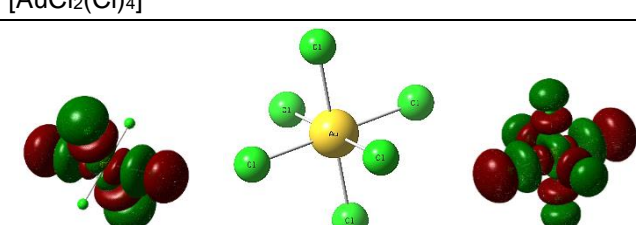
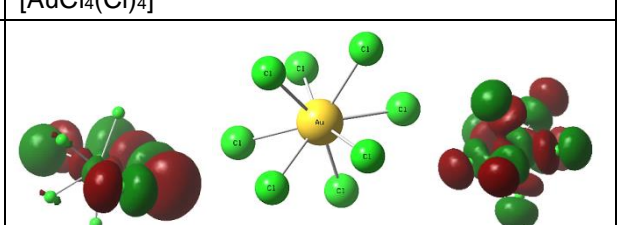
Conversely, a lower gap might also indicate lower kinetic stability for certain reactions due to the facilitated electron transfer events. Furthermore, the potent electron-accepting nature of the electron-accepting group within the $\text{Au}(\text{C}_2\text{H}_4\text{O}_2)_2$ and $\text{Au}(\text{Cl})_4^-$ molecules might be a contributing factor to the observed low gaps [30].

Table 3 shows the molecular structures of the complex with the LUMO and HOMO inclusions.

While a large LUMO-HOMO energy gap is typically associated with increased complex stability and reduced reactivity, a smaller gap shouldn't be solely viewed as a disadvantage. It can offer distinct benefits depending on the desired application. In the context of catalytic reactions involving gold complexes, a smaller LUMO-HOMO gap is favorable. This arises due to the closer proximity of the energy levels between the complex and the reaction participants, facilitating a more facile transfer of electrons. This phenomenon can lead to enhanced catalytic activity, manifesting as faster reaction rates or improved overall efficiency. This effect is particularly noteworthy for the activation of small molecules or processes involving bond breaking and formation. Furthermore, gold complexes characterized by smaller LUMO-HOMO gaps tend to absorb light within the visible region of the electromagnetic spectrum. This property holds significant promise for applications such as photocatalysis, where light serves as the driving force for chemical reactions. Additionally, light-based

sensors that rely on light absorption mechanisms can also benefit from the utilization of such complexes. It is noteworthy that a very small LUMO-HOMO gap has the potential to improve catalytic activity by the activation of small molecules or processes involving bond breaking and formation, and to influence the color of the complex itself by the magnitude of the LUMO-HOMO gap [31,32].

Table 3 Au complexes and their corresponding molecular and LUMO-HOMO structures

Molecular structure / LUMO-HOMO structure	
$\text{AuCl}_2(\text{C}_2\text{H}_4\text{O}_2)_2^{2-}$	$\text{AuCl}_4(\text{C}_2\text{H}_4\text{O}_2)_2^{-}$
	
$[\text{AuCl}_2(\text{Cl})_4]^{2-}$	$[\text{AuCl}_4(\text{Cl})_4]^{-}$
	

While a large LUMO-HOMO energy gap is typically associated with increased complex stability and reduced reactivity, a smaller gap shouldn't be solely viewed as a disadvantage. It can offer distinct benefits depending on the desired application. In the context of catalytic reactions involving gold complexes, a smaller LUMO-HOMO gap is favorable. This arises due to the closer proximity of the energy levels between the complex and the reaction participants, facilitating a more facile transfer of electrons. This phenomenon can lead to enhanced catalytic activity, manifesting as faster reaction rates or improved overall efficiency. This effect is particularly noteworthy for the activation of small molecules or processes involving bond breaking and formation. Furthermore, gold complexes characterized by smaller LUMO-HOMO gaps tend to absorb light within the visible region of the electromagnetic spectrum. This property holds significant promise for applications such as photocatalysis, where light serves as the driving force for chemical reactions. Additionally, light-based sensors that rely on light absorption mechanisms can also benefit from the utilization of such complexes. It is noteworthy that a very small LUMO-HOMO gap has the potential to improve catalytic activity by the activation of small molecules or processes involving bond breaking and formation, and to influence the color of the complex itself by the magnitude of the LUMO-HOMO gap [31,32].

There are several notable implications of this research including to understand how varying pH levels (acidic, neutral, and basic) affect the efficiency of gold extraction using 1:1 Ethaline mixture. By comparing the dissolved gold content (ppm) obtained at each pH level, the maximum pH range (~pH 7-8) for gold leaching with Ethaline was established. Maintaining a consistent acidic environment proved to be challenging due to the need for continuous addition of acetic acid. This resulted in an initial acidic phase, followed by a rise in pH towards neutrality at the 36th hour, and finally, a return to acidic conditions. A positive correlation (correlation coefficient of 0.7046) was observed between pH and ORP values. This indicates that changes in pH influence the oxidation-reduction potential of the leaching solution. The initial low ORP values (first 18 hours) coincided with low gold dissolution rates. Conversely, the highest gold leaching efficiency (42.8%) occurred when ORP reached its peak value at the 64th hour. This suggests a potential link between higher ORP and increased gold dissolution in this specific leaching system, which suggests a potential mechanism for optimizing the leaching

process. Further studies are necessary to confirm this link and explore methods for maintaining a stable and optimal pH-ORP environment for efficient gold extraction.

Further interpolations were executed using MATLAB wherein 4th degree polynomial was employed. It was found that the potential peak should be around 42.5, 45 and 44.5 hours for the neutral, basic and acidic respectively. It was also predicted that an average of 50.5%, 32.3% and 35.9% of gold could be dissolved within those periods. These predictions can serve as a foundation for future studies aimed at experimentally verifying the accuracy of the model.

Experimental findings of this study are supported by the literature on the dissolution mechanism of gold using Ethaline. It was stated that Ethaline promotes a more vigorous gold dissolution reaction, likely due to its high chloride ion concentration. A slightly basic pH (pH 7) yielded the highest gold dissolution efficiency compared to acidic (pH 4) and more basic (pH 10) conditions. This behavior might be attributed to the transformation of the diol component (EG) in Ethaline at high pH. Excessive basicity could lead to reactions that hinder gold dissolution, potentially involving the formation of water or glycerol compounds. These findings align with a previous study on pyrite dissolution, where a similar trend of decreasing extraction efficiency with extremely high pH was observed. For further optimizations, future studies could explore the specific transformations of EG at different pH levels and their impact on the gold dissolution mechanism.

Using the Gaussian software, DFT was employed to interpolate various thermochemical values (e.g., Gibbs energy, LUMO-HOMO energy gap, etc.) based on the proposed reactions. It was found that the $\text{AuCl}_2(\text{C}_2\text{H}_4\text{O}_2)_2^{2-}$ complex, among other gold complexes formed with the ligands of ethylene glycol ($(\text{C}_2\text{H}_4\text{O}_2)_2$ and Cl^-), is the only spontaneous process with a ΔG value of -0.0850332 eV, which is favorable in this case. Other complexes such as $\text{AuCl}_4(\text{C}_2\text{H}_4\text{O}_2)_2^-$, $[\text{AuCl}_2(\text{Cl})_4]^{2-}$ and $[\text{AuCl}_4(\text{Cl})_4]^-$ are non-spontaneous with ΔG values of 1.1267559, 0.3775122 and 0.6525955 eV respectively. The LUMO-HOMO energy gaps are small in general, these indicate high reactivity rates of the complexes, which can be favorable in applications that require fast reaction rates, such as enhancement of a catalysis process and light absorption and color. It is important to acknowledge that the interplay between the LUMO-HOMO gap and these properties is multifaceted and contingent upon the specific molecular structure and the surrounding environmental conditions. These values can be further optimized in the Gaussian software by using the hybrid job type, opt+freq, by testing other functionals, and by performing prior optimizations (e.g., geometry optimizations).

4. CONCLUSION

This study has demonstrated the potential of Ethaline, a deep eutectic solvent composed of choline chloride and ethylene glycol, for the dissolution of gold from sulfidic refractory ores under varying pH conditions. Our findings reveal that Ethaline's performance and the dissolution kinetics of gold are significantly influenced by the pH environment, with the highest gold dissolution observed in near-neutral conditions. The highest gold dissolution was achieved in a neutral pH environment, with a peak dissolution rate of 56.7% at 48 hours, followed by a basic pH environment with a peak dissolution rate of 45.0%. The acidic environment showed a peak dissolution rate of 42.8% at 36 hours, but with fluctuating trends over time.

The present study highlighted the importance of pH control in optimizing the leaching efficiency of Ethaline. The stability of gold complexes and the overall dissolution process were found to be pH-dependent, with neutral and slightly basic conditions providing the most favorable environments for gold recovery. Additionally, the pH-ORP correlation further supported the observed dissolution patterns, where higher ORP values coincided with increased gold dissolution rates.

The use of Ethaline as a leaching agent offers a promising alternative for gold extraction from refractory ores, reducing the environmental impact associated with traditional methods. Future research should focus on scaling up the process and further optimizing the leaching conditions to enhance the applicability of Ethaline in industrial gold recovery operations. This study contributes to the advancement of sustainable mining

practices by providing a viable and less harmful method for gold extraction, aligning with the growing demand for environmentally conscious metallurgical processes.

ACKNOWLEDGEMENTS

The authors would like to thank the Department of Science and Technology - Philippine Council for Industry, Energy and Emerging Technology Research and Development (DOST-PCIEERD), the University of the Philippines, and the Office for Research, Development, and Innovation of the Mapua Malayan Colleges Mindanao for the support throughout the study. The gold ore samples were provided for by Apex Mining Co, Inc. with full permission for the execution of this study.

REFERENCES

- [1] KUBASCHEWSKI, O., VON GOLDBECK, O. *The Thermochemistry of Gold*. Gold Bulletin, 1975, pp. 80–85.
- [2] ROYAL SOCIETY OF CHEMISTRY. *Gold - element information, properties and uses: Periodic Table, Gold - Element information, properties and uses | Periodic Table* [Online].<https://edu.rsc.org/elements/gold/2020010.article>.
- [3] WILLIAMS-JONES, A.E., BOWELL, R.J., MIGDISOV, A.A. *Gold in solution. Elements*. 2009, pp. 281–287.
- [4] *Gold properties: AMNH. American Museum of Natural History* [Online].<https://www.amnh.org/explore/ology/earth/whats-this-gold>.
- [5] ARRIAGADA, F.J., OSSEO-ASARE, K. Gold extraction from refractory ores: Roasting behaviour of pyrite and arsenopyrite. *Precious Metals - Mining, Extraction, and Processing*. 1984, p. 367.
- [6] FRASER, K.S., WALTON, R.H., WELLS, J.A. Processing of refractory gold ores. *Minerals Engineering*. 1991, pp. 7-11.
- [7] DUNN, J.G., CHAMBERLAIN, A.C. The recovery of gold from refractory arsenopyrite concentrates by pyrolysis-oxidation. *Minerals Engineering*. 1997, pp. 919-928.
- [8] WANG, W., HU, X., ZI, F., QIN, X., NIE, Y., ZHANG, Y. Extraction of gold from refractory gold ore using bromate and ferric chloride solution. *Minerals Engineering*. 2019, pp. 89–98.
- [9] ESDAILE, L.J., CHALKER, J.M. The Mercury Problem in Artisanal and Small-Scale Gold Mining. *Chemistry - A European Journal*. 2018, pp. 6905–6916.
- [10] MILLER, J., GARCIA, C. *Solvent extraction reagents for gold recovery from alkaline cyanide solutions*. Salt Lake City, 1993. Department of Metallurgical Engineering, University of Utah.
- [11] ABBOTT, A.P., FRISCH, G. Ionometallurgy: Processing of metals using ionic liquids. *Element Recovery and Sustainability*. 2013, pp. 59–79.
- [12] DIETZ, M.L., HAWKINS, C.A. Metal ion extraction with ionic liquids. *Liquid-Phase Extraction*. 2020, pp. 539–564.
- [13] COULING, D.J., BERNOT, R.J., DOCHERTY, K.M., DIXON, J.K., MAGINN, E.J. Assessing the factors responsible for ionic liquid toxicity to aquatic organisms via quantitative structure–property relationship modeling. *Green Chemistry*. 2006, pp. 82–90.
- [14] WINARDHI, C.W., DA ASSUNCAO GODINHO, J.R., RACHMAWATI, C., ACHIN, I.D., ITURBE, A.U., FRISCH, G., GUTZMER. A particle-based approach to predict the success and selectivity of leaching processes using ethaline - Comparison of simulated and experimental results. *Hydrometallurgy*. 2022, pp. 105869–105869.
- [15] KHAING, S.Y., SUGAI, Y., SASAKI, K. Gold dissolution from ore with iodide-oxidising bacteria. *Scientific Reports*. 2019, p. 4178.
- [16] CUI, X., WANG, Y., WANG, Y., ZHANG, P., LU, W. Extraction of gold based on ionic liquid immobilized in uio-66: An efficient and reusable way to avoid IL loss caused by ion exchange in solvent extraction. *Molecules*. 2023, p. 2165.
- [17] SINGH, M. B., KUMAR, V.S., CHAUDHARY, M., SINGH, P. A mini review on synthesis, properties and applications of deep eutectic solvents. *Journal of the Indian Chemical Society*. 2021, p. 100210.
- [18] LEMAOUI, T., HATAB, F.A., DARWISH, A. S., ATTOUI, A., EL HOUDA HAMMOUDI, N., ALMUSTAFA, G., BENAICHA, M., BENGUERBA, Y., ALNASHEF, I. M. Molecular-based guide to predict the pH of eutectic

- solvents: Promoting an efficient design approach for new green solvents. *ACS Sustainable Chemistry & Engineering*. 2021, pp. 5783–5808.
- [19] ORABY, E.A., EKSTEEN, J.J. Gold dissolution and copper suppression during leaching of copper–gold gravity concentrates in caustic soda-low free cyanide solutions. *Minerals Engineering*. 2016, pp. 10–17.
- [20] ALTINKAYA, P., WANG, Z., KOROLEV, I., HAMUYUNI, J., HAAPALAINEN, M., KOLEHMAINEN, E., YLINIEMI, K., LUNDSTRÖM, M. Leaching and recovery of gold from ore in cyanide-free glycine media. *Minerals Engineering*. 2020, p. 106610.
- [21] TORRES, J., CAMPOS, K.S., HARRISON, C.R. Fluorescently labeling amino acids in a deep eutectic solvent. *Analytical Chemistry*. 2022, pp. 16538–16542.
- [22] TRAN, K.M., RODRIGUES, M.F., KATO, K., BABU, G., AJAYAN, P.M. Deep eutectic solvents for cathode recycling of Li-ion batteries. *Nature energy*. 2019, pp. 339-345.
- [23] ABBOTT, A.P., TTAIB, K.E., FRISCH, G., MCKENZIE, K.J., RYDER, K.S. Electrodeposition of copper composites from deep eutectic solvents based on choline chloride. *Physical Chemistry Chemical Physics*. 2009, pp. 4269-4277.
- [24] WU, J., DING, Y., ZHU, F., GU, Y., WANG, W., SUN, L., MAO, B., YAN, J. The role of water content of deep eutectic solvent ethaline in the anodic process of gold electrode. *Molecules*. 2023, p. 2300.
- [25] TEIMOURI, S., POTGIETER, J.H., BILLING, C., CONRADIE, J. The feasibility of pyrite dissolution in the deep eutectic solvent ethaline: Experimental and theoretical study. *Journal of Molecular Liquids*. 2023, p. 123468.
- [26] MOHAMMADNEJAD, S., PROVIS, J.L., VAN DEVENTER, J.S.J. Computational modelling of interactions between gold complexes and silicates. *Computational and Theoretical Chemistry*. 2017, pp. 113-121.
- [27] OCHTERSKI, J.W. *Thermochemistry in Gaussian*. 2000. Gaussian, Inc.
- [28] XU, B., KONG, W., LI, Q., YANG, Y., JIANG, T., LIU, X. A Review of thiosulfate leaching of gold: Focus on thiosulfate consumption and gold recovery from pregnant solution. *Metals*. 2017, p.222.
- [29] HANSEN, A.S., VOGT, E., KJAERGAARD, H.G. Gibbs energy of complex formation – combining infrared spectroscopy and vibrational theory. *International Reviews in Physical Chemistry*. 2019, pp.115–148.
- [30] MIAR, M., SHIROUDI, A., POURSHAMSIAN, K., OLIAEY, A.R., HATAMJAFARI, F. Theoretical investigations on the HOMO–LUMO gap and global reactivity descriptor studies, natural bond orbital, and nucleus-independent chemical shifts analyses of 3-phenylbenzo[d]thiazole-2(3H)-imine and its para-substituted derivatives: Solvent and substituent effects. *Journal of Chemical Research*. 2020, pp. 147–158.
- [31] WU, Y., YANG, H., GAO, H., HUANG, X., GENG, L., ZHANG, R. Advances in versatile chiral ligands for asymmetric gold catalysis. *Catalysts*. 2023, pp. 1294–1294.
- [32] SHARMA, R., RAGAVAN, K.V., ABHIJITH, K.S., AKANKSHA, A., THAKUR, M.S. Synergistic catalysis by gold nanoparticles and metal ions for enhanced chemiluminescence. *RSC Advances*. 2015, pp. 31434–31438.